ELSEVIER

Contents lists available at ScienceDirect

Extreme Mechanics Letters

journal homepage: www.elsevier.com/locate/eml



Flaw sensitivity of cellulose paper

Qiongyu Chen ^a, Bo Chen ^a, Shuangshuang Jing ^b, Yu Liu ^b, Teng Li ^{a,*}

- ^a Department of Mechanical Engineering, University of Maryland, College Park, MD, 20742, USA
- b Department of Materials Science and Engineering, University of Maryland, College Park, MD, 20742, USA



ARTICLE INFO

Article history: Received 25 May 2022 Received in revised form 29 July 2022 Accepted 2 August 2022 Available online 8 August 2022

Keywords: Cellulose Flaw sensitivity Fractocohesive length Toughness

ABSTRACT

Cellulose is earth-abundant and has exceptional intrinsic mechanical properties. Cellulose-based materials, however, exhibit a large variation in their mechanical properties (e.g., strength, toughness), which calls for the understanding of the sensitivity of these materials to flaws, an area that remains largely unexplored. In this paper, we report a systematic study of the flaw sensitivity of cellulose paper by measuring the fractocohesive lengths of cellulose paper made of cellulose fibers with various diameters (from nanometers to microns) and lengths (from sub-microns to millimeters). Unlike the strength of cellulose paper which depends strongly on the diameter of the constituent cellulose fibers, the flaw sensitivity of cellulose paper is closely related to the aspect ratio (length/diameter) of the cellulose fibers. The larger the aspect ratio of the cellulose fibers, the larger the fractocohesive length, and thus the more flaw tolerant the cellulose paper is. Findings in this paper shed light on designing cellulose-based materials with desirable mechanical performance that is pivotal for the widespread use of this sustainable material.

© 2022 Elsevier Ltd. All rights reserved.

1. Introduction

Cellulose, the most abundant natural polymer in the world, has attracted considerable attention recently owing to its superior mechanical properties [1–3], biodegradability [4,5], and low cost [6,7]. Various cellulose-based materials have been developed, e.g., cellulose-based films (paper) [8,9], hydrogels [10–12], aerogels [13,14], fibers [15], and composites [16,17]. These materials feature a broad range of desirable functions such as optical transparency [18], high strength and toughness [19], programmable hydrophilicity and hydrophobicity [20,21], and electrical/ion/thermal conductivity [22–24], with the potential to be used in diverse applications such as energy storage [25–28], textile engineering [29,30], biomedicine [31–33], and packaging [34].

Among various material forms, cellulose paper is of particular interest as a versatile form to decipher its structure-performance relationship, which in turn sheds light on the design of other cellulose-based materials with desirable properties [35,36]. For example, it has been shown that by decreasing the diameter of the constituent cellulose fibers from microns to nanometers, both the strength and toughness of the resulting cellulose paper can be drastically increased simultaneously, suggesting an anomalous but desirable scaling law to defeat the well-known conflict between strength and toughness [37]. It is also found that the elastic

* Corresponding author. E-mail address: lit@umd.edu (T. Li). modulus of cellulose paper can be enhanced by increasing the packing density and inter-fiber interaction of the cellulose fiber network of the paper [38,39].

To date, existing studies on the mechanics of cellulose-based materials focus on properties such as elastic modulus, strength, toughness, and hardness [40–48]. Despite the superior intrinsic mechanical properties of cellulose, there exist large variations in the mechanical properties of cellulose-based materials. The disparity between the intrinsic mechanical performance of cellulose and that of cellulose-based materials calls for the study of sensitivity to flaws in cellulose-based materials, a topic that remains largely unexplored so far.

Herein, we report a systematic study of the flaw sensitivity of cellulose paper by measuring the fractocohesive lengths of cellulose paper made of cellulose fibers with various diameters (from nanometers to microns) and lengths (from sub-microns to millimeters). Fractocohesive length is a material-specific length defined as the ratio of the fracture energy Γ (in J/m² as measured by rupturing a sample with a long pre-cut) to the work of fracture (in J/m³ as measured by rupturing a sample of no pre-cut) of a material. The fractocohesive length of a material measures the sensitivity of the material to flaws [49–52]. That is, the larger the fractocohesive length, the more flaw tolerant the material is, and vice versa.

Earlier studies demonstrate a strong dependence of the strength of cellulose paper on the diameter of the constituent cellulose fibers, which can be attributed to the reduced defect size in the paper made of finer cellulose fibers [37]. The present

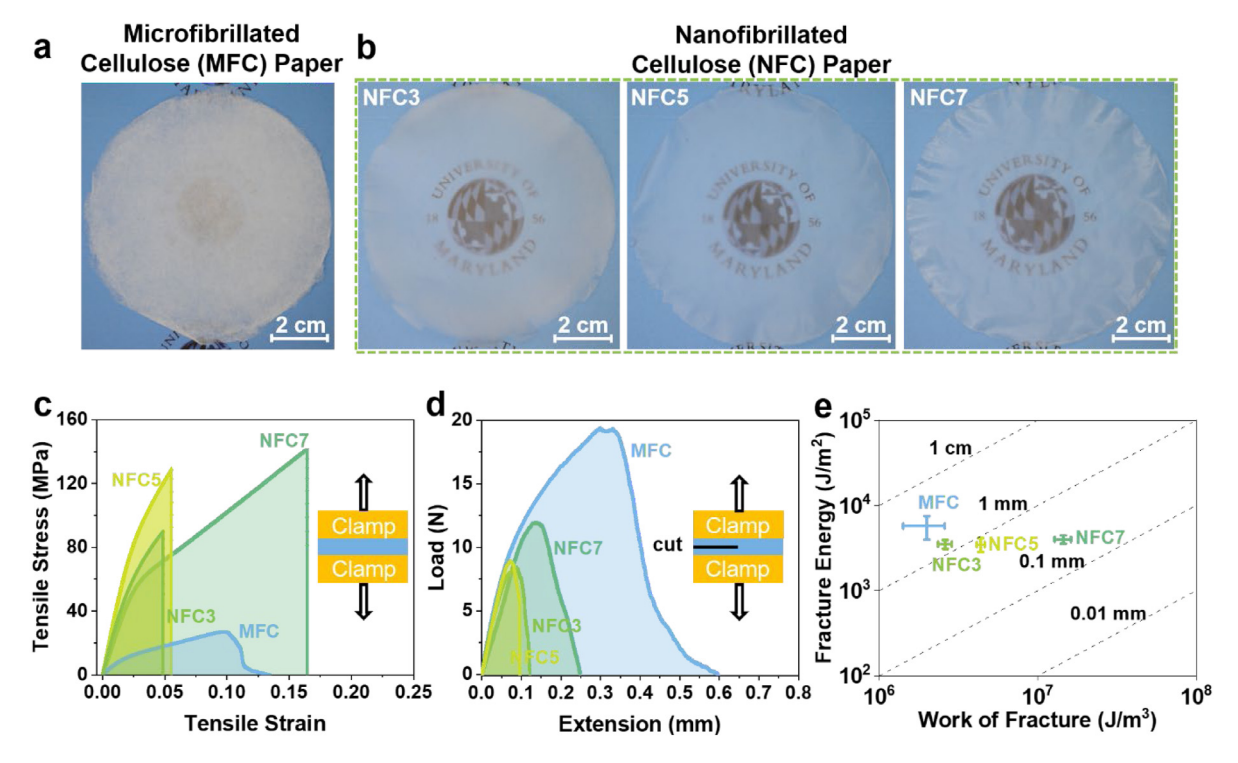


Fig. 1. Photos of (a) microfibrillated cellulose (MFC) paper and (b) nanofibrillated cellulose (NFC) paper prepared by TEMPO treatment using 3 mol, 5 mol, and 7 mol NaClO per kg dried pulp (referred to as NFC3, NFC5, NFC7, respectively), from left to right. (c) Stress-strain curves of the tensile tests of specimens of four types of cellulose paper without pre-cut. The area underneath a curve denotes the work of fracture of the specimen. (d) Load-extension curves of the tensile tests of specimens of four types of cellulose paper with a long pre-cut (half of the specimen width), which is used to measure the fracture energy of the specimen (see Methods). (e) The fracture energy of MFC, NFC3, NFC5, and NFC7 paper is plotted against their corresponding work of fracture. The dashed lines define the contour lines of fractocohesive length.

study reveals that the flaw sensitivity of cellulose paper is closely related to the aspect ratio (length/diameter) of the cellulose fibers, rather than the diameter or the length of the cellulose fibers alone. The larger the aspect ratio of the cellulose fibers, the larger the fractocohesive length, and thus the more flaw tolerant the cellulose paper is. Further characterization finds that the fracture of cellulose paper made of fibers of a large aspect ratio features significant crack bridging in the wake of rupture path, while cellulose paper made of fibers of a small aspect ratio ruptures in a rather brittle nature. The mechanistic understanding of the flaw sensitivity of cellulose paper shed light on designing flaw-tolerant cellulose-based materials, a desirable feature for the widespread use of this sustainable material.

2. Results and discussion

Cellulose paper is prepared by first obtaining a wet "gel cake" from vacuum filtrating ~ 1 wt% cellulose fiber dispersion and then hot pressing it overnight at 60 °C. The dispersion of microfibrillated cellulose (MFC) is prepared by mechanical disintegration of dry wood pulp in deionized water. The resulting MFC paper is shown in Fig. 1a as being nearly opaque (see Methods).

We then conduct oxidation treatment mediated by 2,2,6,6-Tetramethylpiperidine 1-oxyl (TEMPO) to the as-prepared MFC dispersion to disintegrate the micro-sized cellulose fibers down to nanoscale (see Methods) [53]. By controlling the amount of Sodium hypochlorite (NaClO) added to the oxidation treatment (i.e., 3 mol, 5 mol, and 7 mol per kg dried pulp, respectively), we can control the degree of TEMPO oxidation (more NaClO means a higher degree of oxidation) and thus tailor the size (diameter and length) of the resulting nanofibrillated cellulose (NFC). The cellulose paper made of NFC of the above three degrees of TEMPO oxidation is hereafter referred to as NFC3, NFC5, and

NFC7 paper, respectively. As shown in Fig. 1b, as the oxidation degree increases, the resulting NFC paper becomes more and more transparent, which can be attributed to the decreasing diameter of the cellulose fibers well below the wavelengths of visible light [54].

To investigate the mechanical performance of the as-prepared four types of cellulose paper, we perform tensile tests on pristine specimens of cellulose paper with no pre-cut, whose stressstrain curves are plotted in Fig. 1c. The area underneath each curve measures the work of fracture W of the corresponding specimen, in a unit of I/m³. We next perform tensile tests of cellulose paper specimens with a long pre-cut (half of the specimen width), whose load-displacement curves are plotted in Fig. 1d. The fracture energy of the cellulose paper (in a unit of J/m^2) can then be obtained from results in Fig. 1c and d using the method described in [55] (detailed in Methods and Fig. 5). The fracture energy of MFC, NFC3, NFC5, and NFC7 paper is plotted against their corresponding work of fracture in Fig. 1e. The ratio between the fracture energy and work of fracture of each type of paper defines its fractocohesive length. The dashed lines in Fig. 1e define the contour lines of fractocohesive length (with corresponding values labeled). As shown in Figs. 1e and 3d, among the four types of cellulose paper, MFC paper shows the largest fractocohesive length (2.38 mm). For NFC paper, the fractocohesive length is shown to decrease modestly as the degree of TEMPO oxidation increases (1.35 mm for NFC3, 0.80 mm for NFC3, and 0.28 mm for NFC7, respectively).

To understand the parameters that govern the fractocohesive length of cellulose paper, we characterize the length and diameter of the cellulose fibers used to make the four types of cellulose paper, as plotted in Fig. 2. The dimensions of MFC fibers are measured using optical microscopy (Fig. 2a-c) while those of

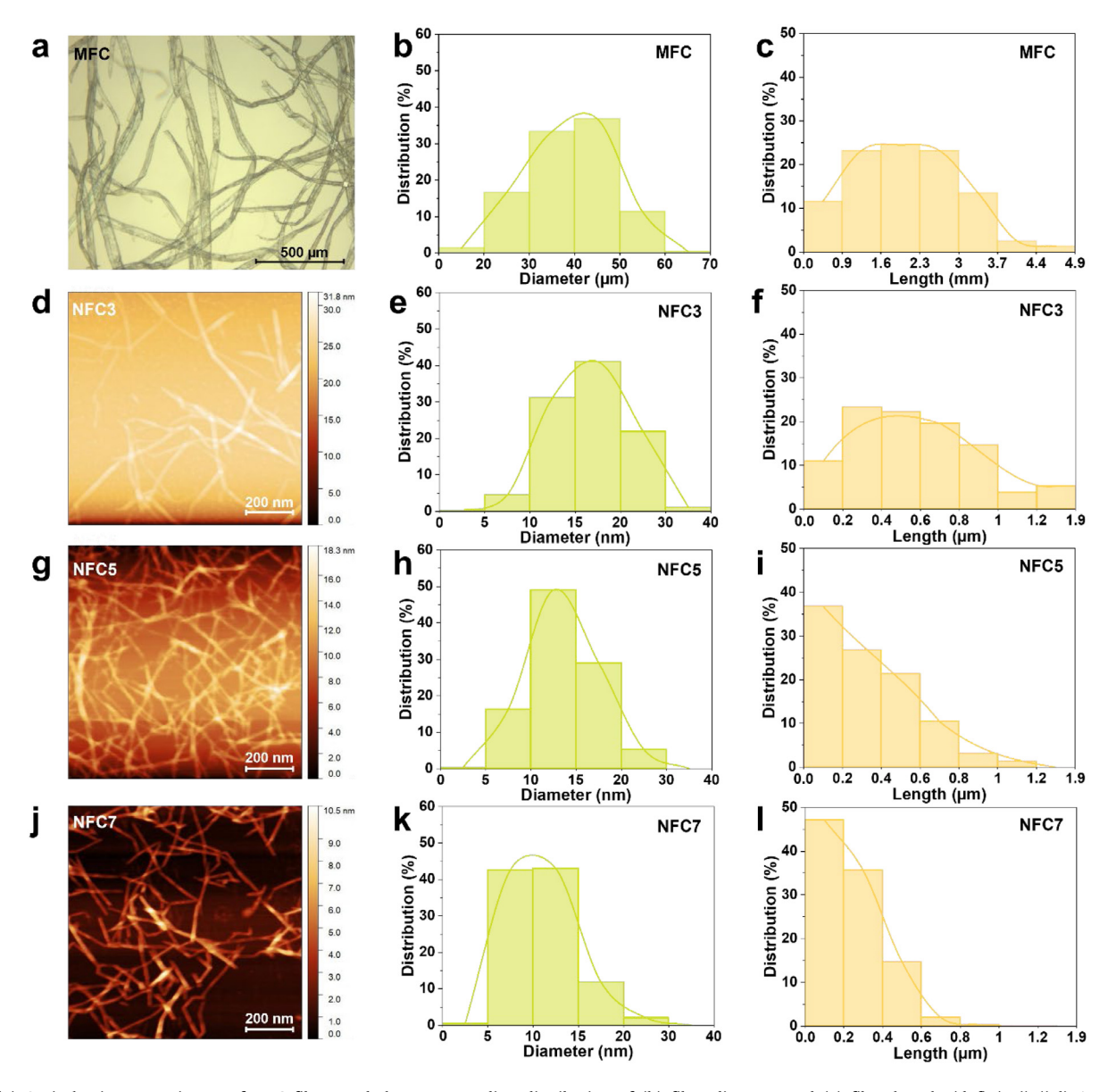


Fig. 2. (a) Optical microscopy image of MFC fibers and the corresponding distribution of (b) fiber diameter and (c) fiber length. (d-f) (g-i) (j-l) Atomic Force Microscopy (AFM) image and the corresponding distribution of fiber diameter and fiber length of NFC3, NFC5, and NFC7 fibers, respectively.

NFC fibers are measured using atomic force microscopy (Fig. 2d-l). The mean values and standard deviations of the length and diameter of the four types of cellulose fiber are listed in Table 1.

It is evident that the TEMPO oxidation treatment effectively disintegrates the MFC fibers into nanoscale and results in a decrease by orders of magnitude in both diameter (from 10 s μm to around 10 nm) and length (from several mm to 100 s nm). For example, the mean diameter of MFC fibers is 3617 times, 6384 times, and 8510 times larger than that of NFC3, NFC5, and NFC7 fibers, respectively. The mean length of MFC fibers is 2298 times, 2850 times, and 3464 times larger than that of NFC3, NFC5, and NFC7 fibers, respectively. As the degree of TEMPO oxidation increases, the diameter and length of the resulting NFC fibers decrease modestly, which can be attributed to the increasing number of carboxyl groups introduced to the cellulose fibers to facilitate fibrilization [53,56] and decreasing degree of polymerization of cellulose chains [57,58], respectively.

Fig. 3a–c compare the tensile strength, work of fracture, and fracture energy of the four types of cellulose paper made of MFC, NFC3, NFC5, and NFC7, respectively. As the mean diameter of the

constituent cellulose fibers decreases from 39.25 µm for MFC to 17.08 nm for NFC3, 13.77 nm for NFC5, and 11.33 nm for NFC7, the tensile strength of the cellulose paper increases from 29.20 MPa to 90.96 MPa (3.12 times higher), 129.95 MPa (4.25 times higher), and 145.11 MPa (4.97 times higher), respectively. Such a dependence of the tensile strength of cellulose paper on the diameter of cellulose fiber can be attributed to the decrease in defect size in the paper as the constituent fibers become thinner. The work of fracture measures the energy dissipation during the rupture of the specimen and is shown to increase as the diameter of the cellulose fibers decreases, which can be understood by the nature of the failure mechanism of the cellulose paper. The rupture of cellulose paper results from relative sliding among neighboring cellulose fibers. Such a sliding process features a cascade of events of forming, breaking, and reforming hydrogen bonds between neighboring cellulose fibers in the paper, the dominant mechanism of energy dissipation during the rupture of the paper [37]. The smaller the diameter of the cellulose fibers, the larger the surface area of the cellulose fibers, and thus the higher the number of hydrogen bonds that can contribute to the

Table 1Dimensions of the four types of cellulose fibers.

	MFC (μm)	NFC3 (nm)	NFC5 (nm)	NFC7 (nm)
Lengtha	2074.01 ± 938.98	573.25 ± 319.05	324.86 ± 251.34	243.71 ± 151.74
Diameter ^a	39.25 ± 9.07	17.08 ± 4.99	13.77 ± 3.97	11.33 ± 3.5

 $^{^{}a}$ Mean \pm standard deviation.

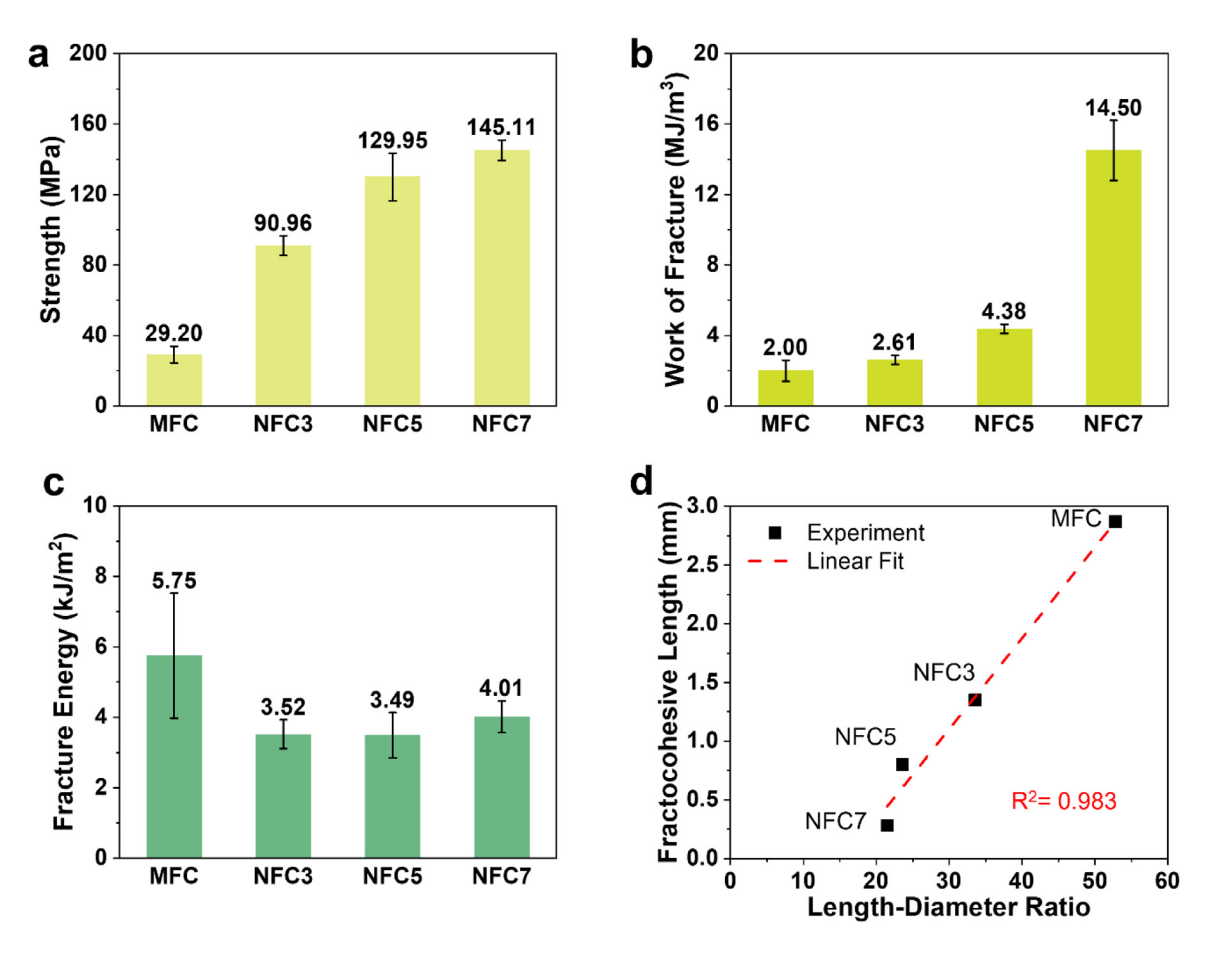


Fig. 3. Comparison of the mechanical properties of the four types of cellulose papers: (a) tensile strength, (b) work of fracture, (c) fracture energy. (d) plots the fractocohesive length of the four types of cellulose paper against the length-diameter ratio of the corresponding constituent cellulose fibers, which shows a linear dependence with a goodness-of-fit measure of $R^2 = 0.983$.

energy dissipation as the cellulose paper ruptures. Fig. 3c shows the fracture energies of the four types of cellulose papers, where MFC paper exhibits the highest fracture energy over NFC papers, which can be attributed to the significant crack bridging effect of the MFC fibers during fracture.

The ratio between the fracture energy and work of fracture of the cellulose paper defines its fractocohesive length, which is plotted in Fig. 3d for the four types of cellulose paper against the corresponding length-to-diameter ratio of the constituent cellulose fibers. A linear dependence of the fractocohesive length of cellulose paper on the aspect ratio of cellulose fibers emerges, with a goodness-of-fit measure of $R^2 = 0.983$. It is worth noting that, even as the TEMPO oxidation leads to a decrease of three orders of magnitude in both the diameter and length of the cellulose fiber, the fractocohesive lengths of the resulting cellulose paper only decrease from 2.87 mm for MFC paper to 1.35 mm for NFC3 paper (2.16 times lower), 0.80 mm for NFC5 paper (3.59 times lower), and 0.28 mm for NFC7 paper (10.25 times lower), respectively. In other words, the fractocohesive length of cellulose paper is closely related to the aspect ratio of the cellulose fibers, rather than the diameter or the length of the cellulose fibers alone.

To further illustrate the difference in the rupture behavior of cellulose paper made of cellulose fibers of different sizes, Fig. 4a and b compare the failure process of an MFC paper specimen and an NFC3 paper specimen under tension. A pre-cut of the length of the half-width of the specimen is introduced before applying the tensile loading in both specimens. As the applied tensile strain increases, the pre-cut in the MFC paper opens up. The increasing stress level near the tip of the pre-cut leads to substantial relative sliding of the MFC fibers around the tip. Given that the mean length of MFC fibers (2.07 mm) is significantly larger than the crack opening ($\sim\!96~\mu m$), the MFC fibers ahead of the crack tip can effectively blunt the initially sharp tip of the pre-cut, as evident in Fig. 4a. Further propagation of the crack features a substantial bridging effect of the MFC fibers along the crack path, leading to a rather gradual rupture process.

By contrast, the tensile rupture of the NFC paper with a precut is a brittle manner. As the applied tensile strain increases, the sharp pre-cut results in stress concentration near its tip, driving an abrupt propagation of the pre-cut along its initial direction and leading to the rupture of the specimen. The crack opening during the rupture process is significantly smaller than that in the MFC paper. Zoom-in photo in Fig. 4b shows a smooth crack surface of

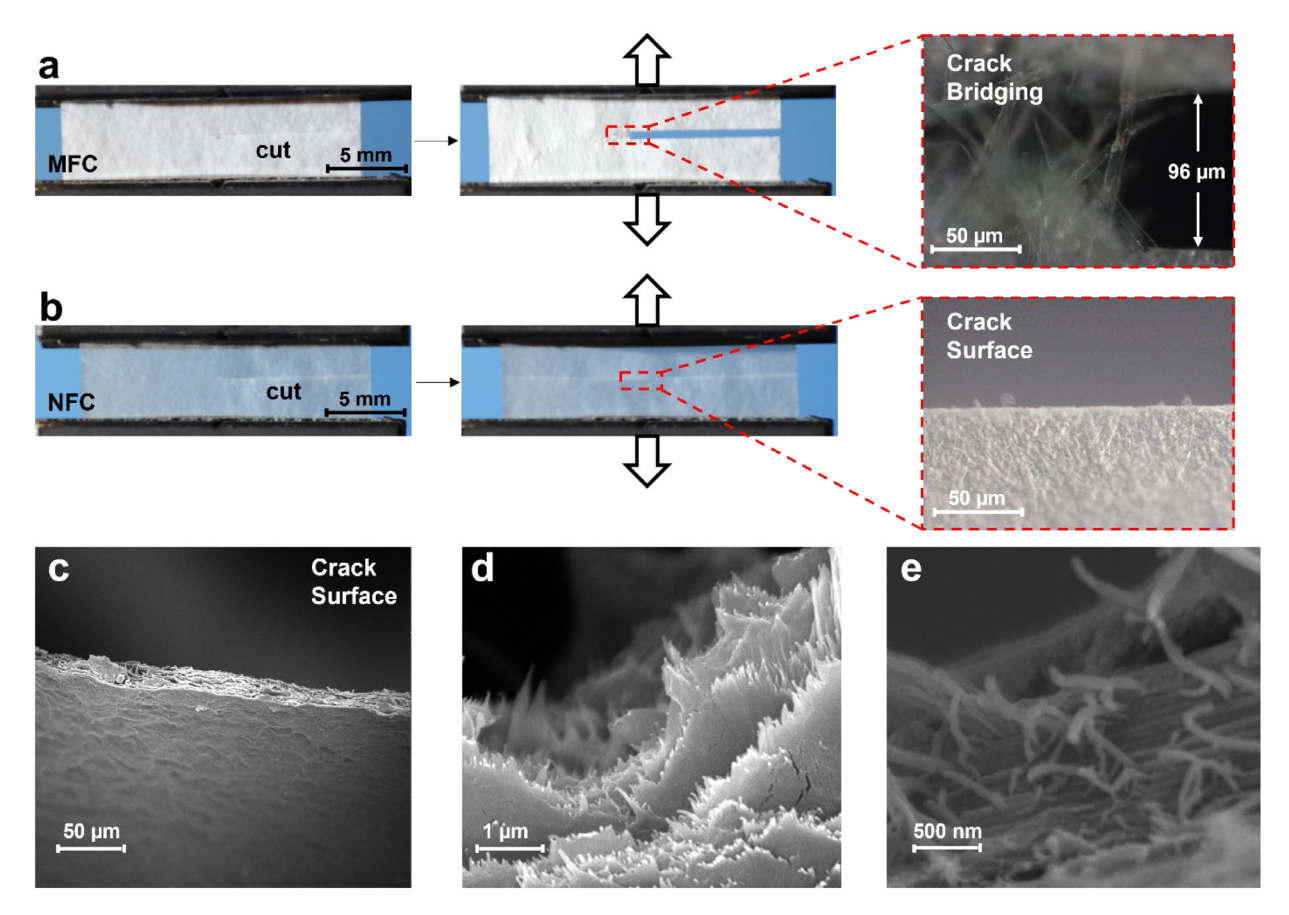


Fig. 4. Comparison of tensile rupture behavior of (a) MFC paper and (b) NFC paper. The left and middle panels show the optical photos of the specimen before and after tension is applied. Zoom-in optical photos reveal distinct rupture behaviors of MFC paper (featuring significant crack bridging by the long cellulose fibers) and NFC paper (in a brittle manner with a rather smooth crack surface). Photos of NFC3 paper are shown in (b). Similar rupture behavior is also observed in NFC5 and NFC7 paper. (c-e) SEM images of the crack surface of NFC3 paper in (b) further reveal the fracture behavior.

the ruptured NFC paper, without appreciable crack bridging by the NFC fibers, in sharp contrast with the rupture process of the MFC paper. All three types of NFC paper are shown to have similar brittle rupture behavior under tension. Further characterization via Scanning Electron Microscopy (SEM) on the crack surface of NFC paper in Fig. 4c-e shows that even though fiber pullout is evident at the crack surface, the great reduction in both length and diameter of the fiber leads to a rather trivial and negligible crack bridging effect, explaining the brittle rupture behavior of NFC paper.

3. Conclusions

In summary, we investigate the flaw sensitivity of cellulose paper by measuring the fractocohesive lengths of cellulose paper made of cellulose fibers with various diameters (from nanometers to microns) and lengths (from sub-microns to millimeters). We find that the fractocohesive length of fiber-constituted cellulose paper is dependent on the aspect ratio (length/diameter) of the cellulose fibers in a linear fashion. The larger the aspect ratio of the cellulose fibers, the larger the fractocohesive length, and thus the more flaw tolerant the cellulose paper is. Further investigations are desirable to better understand the dependence of fractocohesive length of cellulose paper synthesized via different methods on the dimension of the constituent fibers.

Methods

• Preparation of microfibrillated cellulose (MFC)

5 g of Kraft bleached softwood pulp (*International Paper*, *USA*) is immersed in 300 mL DI water and stirred harshly overnight by

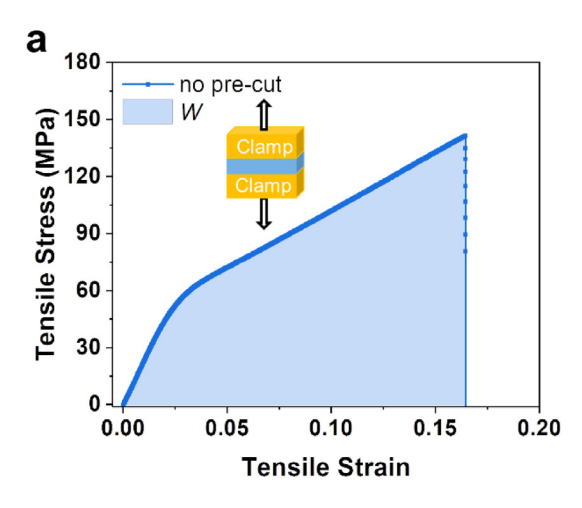
RW 20 Digital (*IKA-Werke*, *Germany*) to obtain the mechanically disintegrated MFC solution.

• Preparation of nanofibrillated cellulose (NFC)

First, 0.1 mol of 2,2,6,6-Tetramethylpiperidine 1-oxyl (TEMPO) (Sigma-Aldrich) per kg dried pulp, 1 mol of sodium bromide (NaBr) per kg dried pulp are added into 300 mL MFC solution and stirred for 20 min. Then, a certain amount Sodium hypochlorite (NaClO) is added into the mixture dropwise to initiate TEMPO oxidation of the cellulose under stirring. The amounts of NaClO are 3 mol, 5 mol, 7 mol NaClO per kg dried pulp for NFC3, NFC5, and NFC7, respectively. During the reaction process, the pH of the solution is maintained at 10.5 by dropwise adding 3 mol/L of NaOH. The reaction ends when NaClO is fully consumed. After TEMPO treatment, the fibers are washed thoroughly with distilled water and disintegrated into NFC by one pass through a Nano DeBEE Laboratory Homogenizer (BEE International, USA). The NFC dispersion is obtained with a content of 1 wt% by weight.

• Preparation of cellulose paper

Around 250 mL cellulose fiber dispersion (with a constant mass content of 0.19 g) is poured into the filtration apparatus containing a nitrocellulose ester filter membrane with 0.65- μ m pore size. The filtration time varies from 15 min to 3.5 h depending on the cellulose fiber diameter. After filtration, a strong gel forms on top of the filter membrane. This gel "cake" is sandwiched between two smooth filter membranes and twelve filter papers and compressed overnight at 60 °C under a pressure of 10 MPa by a hot press machine (*YLJ-HP300, MTI*). The resulting cellulose paper is \sim 90 mm in diameter, 15 \sim 25 μ m in thickness, and 1.04 \sim 1.32 g/cm³ in density.



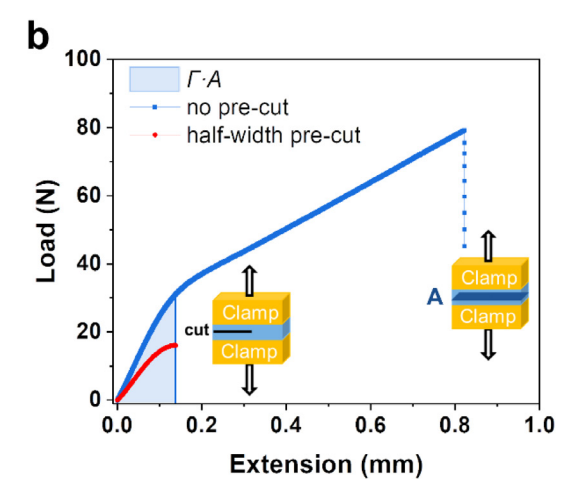


Fig. 5. Measurement of fractocohesive length (Γ/W) of cellulose paper. (a) A typical stress-strain curve of a specimen with no pre-cut, the area underneath the curve defines the work of fracture W (J/m^3); (b) Load–extension curves of specimens with no pre-cut (blue) and with a half-width pre-cut (red). The partial area under the former load–extension curve up to the corresponding critical extension (the extension at the maximum load) of the latter load–extension curve defines the product of fracture energy Γ and the cross-sectional area A of the specimen with no pre-cut. (For interpretation of the references to color in this figure legend, the reader is referred to the web version of this article.)

• Materials characterization

The morphology of NFC fibers is obtained utilizing an Atomic Force Microscope (*Cypher ES Environmental AFM, Oxford Instruments*) in tapping mode. The dimensions of NFC fibers are collected by the software *Gwyddion*. The morphology of MFC fibers as well as the crack surface of MFC paper are obtained utilizing an optical microscope (*Olympus Accura Zoom BX30*) with both bright and cross-polarized light illuminations. The dimensions of MFC fibers are collected by software *INFINITY ANALYZE*. The morphologies of the crack surface of cellulose papers are characterized by Tescan XEIA3 SEM. The SEM samples are processed by gold sputtering before the test.

• Mechanical tests

Mechanical tests are conducted on an Instron 5940 Series Single Column Table Frames with a 1000 N load cell and a nominal displacement rate of 0.1 mm/min. Specimens are cut into a 25 mm by 20 mm rectangle from cellulose paper (see insets of Fig. 5a). Half-width pre-cuts on specimens are introduced by a sharp razor for determination of fracture energy (see insets of Fig. 5b). The initial grip distance is set as 5 mm to ensure the ratio between the grip distance and the sample thickness is \sim 200:1. At least ten specimens were measured for each type of cellulose paper. Fig. 5 explains how the fractocohesive length of cellulose paper is measured. The work of fracture W is measured by the area underneath the stress-strain curve of a specimen with no pre-cut, as shown in Fig. 5a. The fracture energy Γ is determined by comparing two load-extension curves; one is from a specimen with no pre-cut, the other is from a specimen with a half-width pre-cut, as shown in Fig. 5b. The partial area under the former load-extension curve up to the corresponding critical extension (the extension at the maximum load) of the latter loadextension curve defines the product of fracture energy Γ and the cross-sectional area A of the specimen with no pre-cut. The ratio between fracture energy and work of fracture defines the fractocohesive length (Γ/W) of cellulose paper.

CRediT authorship contribution statement

Qiongyu Chen: Methodology, Investigation, Data processing, Validation, Formal analysis, Visualization, Writing – original draft, Writing – review & editing. **Bo Chen:** Methodology, Investigation. **Shuangshuang Jing:** Methodology, Investigation. **Yu Liu:**

Methodology. **Teng Li:** Conceptualization, Methodology, Investigation, Supervision, Writing – reviewing & editing.

Declaration of competing interest

The authors declare that they have no known competing financial interests or personal relationships that could have appeared to influence the work reported in this paper.

Data availability

Data will be made available on request.

Acknowledgments

This research is supported by the National Science Foundation, USA (Grants CMMI # 1936452). We acknowledge the support of the Maryland Nanocenter and its Surface Analysis Center. We also thank International Paper, USA, for providing the Kraft softwood pulp (bleached) as cellulose source material. Qiongyu Chen acknowledges the support from Dean's Fellowship at the A. James Clark School of Engineering, USA and the UMD Graduate School Summer Research Fellowship, USA.

References

- R.J. Moon, A. Martini, J. Nairn, J. Simonsen, J. Youngblood, Cellulose nanomaterials review: Structure, properties and nanocomposites, 2011, http://dx.doi.org/10.1039/c0cs00108b.
- [2] U. Ray, S. Zhu, Z. Pang, T. Li, Mechanics design in cellulose-enabled high-performance functional materials, 2020, pp. 1–22, http://dx.doi.org/ 10.1002/adma.202002504, 2002504.
- [3] T. Li, EML webinar overview: Advanced materials toward a sustainable future—Mechanics design, Extreme Mech. Lett. 42 (2021) 101107, http://dx.doi.org/10.1016/j.eml.2020.101107.
- A. Sannino, C. Demitri, M. Madaghiele, Biodegradable cellulose-based hydrogels: design and applications, Materials (Basel) 2 (2009) 353–373, http://dx.doi.org/10.3390/ma2020353.
- [5] X. Wang, Q. Xia, S. Jing, C. Li, Q. Chen, B. Chen, Z. Pang, B. Jiang, W. Gan, G. Chen, M. Cui, L. Hu, T. Li, Strong, hydrostable, and degradable straws based on cellulose-lignin reinforced composites, Small 2008011 (2021) 1–10, http://dx.doi.org/10.1002/smll.202008011.
- [6] H. Tu, M. Zhu, B. Duan, L. Zhang, Recent progress in high-strength and robust regenerated cellulose materials, Adv. Mater. 2000682 (2020) 1–22, http://dx.doi.org/10.1002/adma.202000682.

- [7] Z. Hussain, W. Sajjad, T. Khan, F. Wahid, Production of bacterial cellulose from industrial wastes: a review, Cellulose 26 (2019) 2895–2911, http: //dx.doi.org/10.1007/s10570-019-02307-1.
- [8] M. Henriksson, L.A. Berglund, P. Isaksson, T. Lindström, T. Nishino, Cellulose nanopaper structures of high toughness, Biomacromolecules 9 (2008) 1579–1585, http://dx.doi.org/10.1021/bm800038n.
- [9] M. Zhu, Y. Wang, S. Zhu, L. Xu, C. Jia, J. Dai, J. Song, Y. Yao, Y. Wang, Y. Li, D. Henderson, W. Luo, H. Li, M.L. Minus, T. Li, L. Hu, Anisotropic, transparent films with aligned cellulose nanofibers, Adv. Mater. 29 (2017) http://dx.doi.org/10.1002/adma.201606284.
- [10] M. Chen, J. Chen, W. Zhou, J. Xu, C.P. Wong, High-performance flexible and self-healable quasi-solid-state zinc-ion hybrid supercapacitor based on borax-crosslinked polyvinyl alcohol/nanocellulose hydrogel electrolyte, J. Mater. Chem. A 7 (2019) 26524–26532, http://dx.doi.org/10.1039/c9ta10944g.
- [11] Y. Kuang, C. Chen, J. Cheng, G. Pastel, T. Li, J. Song, F. Jiang, Y. Li, Y. Zhang, S.H. Jang, G. Chen, T. Li, L. Hu, Selectively aligned cellulose nanofibers towards high-performance soft actuators, Extreme Mech. Lett. 29 (2019) 100463, http://dx.doi.org/10.1016/j.eml.2019.100463.
- [12] Q. Ding, X. Xu, Y. Yue, C. Mei, C. Huang, S. Jiang, Q. Wu, J. Han, Nanocellulose-mediated electroconductive self-healing hydrogels with high strength, plasticity, viscoelasticity, stretchability, and biocompatibility toward multifunctional applications, ACS Appl. Mater. Interfaces 10 (2018) 27987–28002, http://dx.doi.org/10.1021/acsami.8b09656.
- [13] J. Garemark, X. Yang, X. Sheng, O. Cheung, L. Sun, L.A. Berglund, Y. Li, Top-down approach making anisotropic cellulose aerogels as universal substrates for multifunctionalization, 2020, http://dx.doi.org/10.1021/acsnano.0c01888
- [14] C. Chen, J. Song, S. Zhu, Y. Li, Y. Kuang, J. Wan, D. Kirsch, L. Xu, Y. Wang, T. Gao, Y. Wang, H. Huang, W. Gan, A. Gong, T. Li, J. Xie, L. Hu, Scalable and sustainable approach toward highly compressible, anisotropic, lamellar carbon sponge, Chem. 4 (2018) 544–554, http://dx.doi.org/10.1016/j.chempr.2017.12.028.
- [15] Y. Li, H. Zhu, Y. Wang, U. Ray, S. Zhu, J. Dai, C. Chen, K. Fu, S.-H. Jang, D. Henderson, T. Li, L. Hu, Cellulose-nanofiber-enabled 3D printing of a carbon-nanotube microfiber network, Small Methods 1 (2017) 1700222, http://dx.doi.org/10.1002/smtd.201700222.
- [16] S. Venkatarajan, A. Athijayamani, An overview on natural cellulose fiber reinforced polymer composites, Mater. Today Proc. 37 (2021) 3620–3624, http://dx.doi.org/10.1016/J.MATPR.2020.09.773.
- [17] Y. Zhou, C. Chen, S. Zhu, C. Sui, C. Wang, Y. Kuang, U. Ray, D. Liu, A. Brozena, U.H. Leiste, N. Quispe, H. Guo, A. Vellore, H.A. Bruck, A. Martini, B. Foster, J. Lou, T. Li, L. Hu, A printed, recyclable, ultra-strong, and ultra-tough graphite structural material, Mater. Today 30 (2019) 17–25, http://dx.doi.org/10.1016/J.MATTOD.2019.03.016.
- [18] Z. Fang, H. Zhu, Y. Yuan, D. Ha, S. Zhu, C. Preston, Q. Chen, Y. Li, X. Han, S. Lee, Novel nanostructured paper with ultrahigh transparency and ultrahigh haze for solar cells, Nano Lett. 14 (2014) 765–773, http://dx.doi.org/10.1021/nl404101p.
- [19] J. Song, C. Chen, S. Zhu, M. Zhu, J. Dai, U. Ray, Y. Li, Y. Kuang, Y. Li, N. Quispe, Y. Yao, A. Gong, U.H. Leiste, H.A. Bruck, J.Y. Zhu, A. Vellore, H. Li, M.L. Minus, Z. Jia, A. Martini, T. Li, L. Hu, Processing bulk natural wood into a high-performance structural material, Nature 554 (2018) 224–228, http://dx.doi.org/10.1038/nature25476.
- [20] F. Rol, M.N. Belgacem, A. Gandini, J. Bras, Recent advances in surface-modified cellulose nanofibrils, Prog. Polym. Sci. 88 (2019) 241–264, http://dx.doi.org/10.1016/J.PROGPOLYMSCI.2018.09.002.
- [21] D.W. Wei, H. Wei, A.C. Gauthier, J. Song, Y. Jin, H. Xiao, Superhydrophobic modification of cellulose and cotton textiles: Methodologies and applications, J. Bioresour. Bioprod. 5 (2020) 1–15, http://dx.doi.org/10.1016/J. JOBAB.2020.03.001.
- [22] Y. Zhou, C. Chen, X. Zhang, D. Liu, L. Xu, J. Dai, S.C. Liou, Y. Wang, C. Li, H. Xie, Q. Wu, B. Foster, T. Li, R.M. Briber, L. Hu, Decoupling ionic and electronic pathways in low-dimensional hybrid conductors, J. Am. Chem. Soc. 141 (2019) 17830–17837, http://dx.doi.org/10.1021/jacs.9b09009.
- [23] G. Zu, S. Zeng, B. Yang, J. Huang, Transparent, ultraflexible, and superinsulating nanofibrous biocomposite aerogelsviaambient pressure drying, J. Mater. Chem. A 9 (2021) 5769–5779, http://dx.doi.org/10.1039/d0ta12244k.
- [24] M.N. Azman Mohammad Taib, T.S. Hamidon, Z.N. Garba, D. Trache, H. Uyama, M.H. Hussin, Recent progress in cellulose-based composites towards flame retardancy applications, Polymer (Guildf.) 244 (2022) 124677, http://dx.doi.org/10.1016/J.POLYMER.2022.124677.
- [25] Y. Li, H. Zhu, F. Shen, J. Wan, S. Lacey, Z. Fang, H. Dai, L. Hu, Nanocellulose as green dispersant for two-dimensional energy materials, Nano Energy 13 (2015) 346–354, http://dx.doi.org/10.1016/j.nanoen.2015.02.015.
- [26] J. Chen, K. Fang, Q. Chen, J. Xu, C.P. Wong, Integrated paper electrodes derived from cotton stalks for high-performance flexible supercapacitors, Nano Energy 53 (2018) 337–344, http://dx.doi.org/10.1016/j.nanoen.2018. 08.056.

- [27] Z. Wang, Y. Lee, S. Kim, J. Seo, S. Lee, L. Nyholm, Why cellulose-based electrochemical energy storage devices?, 2020, pp. 1–18, http://dx.doi.org/ 10.1002/adma.202000892, 2000892.
- [28] J. Qian, Q. Chen, M. Hong, W. Xie, S. Jing, Y. Bao, G. Chen, Z. Pang, L. Hu, T. Li, Toward stretchable batteries: 3D-printed deformable electrodes and separator enabled by nanocellulose, Mater. Today (2022) http://dx.doi.org/ 10.1016/J.MATTOD.2022.02.015.
- [29] W. Sajjad, F. He, M.W. Ullah, M. Ikram, Fabrication of bacterial cellulosecurcumin nanocomposite as a novel dressing for partial thickness skin burn, 8 (2020) 1–12. http://dx.doi.org/10.3389/fbioe.2020.553037.
- [30] A.P. Provin, V.O. dos Reis, S.E. Hilesheim, R.T. Bianchet, A.R. de Aguiar Dutra, A.L.V. Cubas, Use of bacterial cellulose in the textile industry and the wettability challenge—a review, Cellulose 28 (2021) 8255–8274, http://dx.doi.org/10.1007/s10570-021-04059-3.
- [31] A.B. Seabra, J.S. Bernardes, W.J. Fávaro, A.J. Paula, N. Durán, Cellulose nanocrystals as carriers in medicine and their toxicities: A review, Carbohydr. Polym. 181 (2018) 514–527, http://dx.doi.org/10.1016/J.CARBPOL. 2017.12.014.
- [32] T. Aziz, A. Ullah, H. Fan, R. Ullah, F. Haq, F.U. Khan, M. Iqbal, J. Wei, Cellulose nanocrystals applications in health, medicine and catalysis, J. Polym. Environ. 29 (2021) 2062–2071, http://dx.doi.org/10.1007/s10924-021-02045-1.
- [33] J. Kucińska-Lipka, I. Gubanska, H. Janik, Bacterial cellulose in the field of wound healing and regenerative medicine of skin: recent trends and future prospectives, Polym. Bull. 72 (2015) 2399–2419, http://dx.doi.org/10.1007/ s00289-015-1407-3.
- [34] P. Cazón, M. Vázquez, Bacterial cellulose as a biodegradable food packaging material: A review, Food Hydrocoll. 113 (2021) 106530, http://dx.doi.org/ 10.1016/J.FOODHYD.2020.106530.
- [35] C. Chen, Structure-property-function relationships of natural and engineered wood, Nat. Rev. Mater. 19–21. http://dx.doi.org/10.1038/s41578-020-0195-z.
- [36] Y.Z. Hou, Q.F. Guan, J. Xia, Z.C. Ling, Z.Z. He, Z.M. Han, H. Bin Yang, P. Gu, Y.B. Zhu, S.H. Yu, H.A. Wu, Strengthening and toughening hierarchical nanocellulose via humidity-mediated interface, ACS Nano 15 (2021) 1310–1320, http://dx.doi.org/10.1021/acsnano.0c08574.
- [37] H. Zhu, S. Zhu, Z. Jia, S. Parvinian, Y. Li, O. Vaaland, L. Hu, T. Li, Anomalous scaling law of strength and toughness of cellulose nanopaper, Proc. Natl. Acad. Sci. USA 112 (2015) 8971–8976, http://dx.doi.org/10.1073/ pnas.1502870112.
- [38] R. Mao, S. Goutianos, W. Tu, N. Meng, S. Chen, T. Peijs, Modelling the elastic properties of cellulose nanopaper, Mater. Des. 126 (2017) 183–189, http://dx.doi.org/10.1016/j.matdes.2017.04.050.
- [39] S. Lavrykov, S.B. Lindström, K.M. Singh, B.V. Ramarao, 3D network simulations of paper structure, Nord. Pulp Pap. Res. J. 27 (2012) 256–263, http://dx.doi.org/10.3183/NPPRJ-2012-27-02-p256-263.
- [40] Q. Meng, B. Li, T. Li, X.Q. Feng, Effects of nanofiber orientations on the fracture toughness of cellulose nanopaper, Eng. Fract. Mech. 194 (2018) 350–361, http://dx.doi.org/10.1016/j.engfracmech.2018.03.034.
- [41] Q. Meng, T.J. Wang, Mechanics of strong and tough cellulose nanopaper, Appl. Mech. Rev. 71 (2019) 1–30, http://dx.doi.org/10.1115/1.4044018.
- [42] Q. Meng, B. Li, T. Li, X.Q. Feng, A multiscale crack-bridging model of cellulose nanopaper, J. Mech. Phys. Solids 103 (2017) 22–39, http://dx.doi. org/10.1016/j.jmps.2017.03.004.
- [43] Q. Meng, X. Shi, A microstructure-based constitutive model of anisotropic cellulose nanopaper with aligned nanofibers, Extreme Mech. Lett. 43 (2021) 101158, http://dx.doi.org/10.1016/j.eml.2020.101158.
- [44] Z. Li, W. Xia, Coarse-grained modeling of nanocellulose network towards understanding the mechanical performance, Extreme Mech. Lett. 40 (2020) 100942, http://dx.doi.org/10.1016/j.eml.2020.100942.
- [45] Z. Li, Y. Liao, Y. Zhang, Y. Zhang, W. Xia, Microstructure and dynamics of nanocellulose films: Insights into the deformational behavior, Extreme Mech. Lett. 50 (2022) 101519, http://dx.doi.org/10.1016/j.eml.2021.101519.
- [46] U. Ray, Z. Pang, T. Li, Mechanics of cellulose nanopaper using a scalable coarse-grained modeling scheme, Cellulose 28 (2021) 3359–3372, http: //dx.doi.org/10.1007/s10570-021-03740-x.
- [47] B. Chen, U.H. Leiste, Q. Chen, W.L. Fourney, T. Li, Correlation between rockwell and brinell hardness measurements, J. Appl. Mech. 89 (2022) http://dx.doi.org/10.1115/1.4054094.
- [48] B. Chen, U.H. Leiste, W.L. Fourney, Y. Liu, Q. Chen, T. Li, Hardened wood as a renewable alternative to steel and plastic, Matter. 4 (2021) 3941–3952, http://dx.doi.org/10.1016/j.matt.2021.09.020.
- [49] C. Yang, T. Yin, Z. Suo, Polyacrylamide hydrogels. I. Network imperfection, J. Mech. Phys. Solids 131 (2019) 43–55, http://dx.doi.org/10.1016/j.jmps. 2019.06.018.
- [50] Y. Zhou, J. Hu, P. Zhao, W. Zhang, Z. Suo, T. Lu, Flaw-sensitivity of a tough hydrogel under monotonic and cyclic loads, J. Mech. Phys. Solids 153 (2021) 104483, http://dx.doi.org/10.1016/J.JMPS.2021.104483.
- [51] C. Li, Z. Wang, Y. Wang, Q. He, R. Long, S. Cai, Effects of network structures on the fracture of hydrogel, Extreme Mech. Lett. 49 (2021) 101495, http: //dx.doi.org/10.1016/J.EML.2021.101495.

- [52] C. Chen, Z. Wang, Z. Suo, Flaw sensitivity of highly stretchable materials, Extreme Mech. Lett. 10 (2017) 50–57, http://dx.doi.org/10.1016/j.eml.2016. 10 002
- [53] A. Isogai, T. Saito, H. Fukuzumi, TEMPO-oxidized cellulose nanofibers, Nanoscale 3 (2011) 71-85, http://dx.doi.org/10.1039/c0nr00583e.
- [54] H. Zhu, S. Parvinian, C. Preston, O. Vaaland, Z. Ruan, L. Hu, Transparent nanopaper with tailored optical properties, Nanoscale 5 (2013) 3787–3792, http://dx.doi.org/10.1039/c3nr00520h.
- [55] R.S. Rivlin, A.G. Thomas, Rupture of rubber. I., Characteristic energy for tearing, J. Polym. Sci. 10 (1953) 291–318, http://dx.doi.org/10.1002/pol. 1953.120100303.
- [56] T. Saito, S. Kimura, Y. Nishiyama, A. Isogai, Cellulose nanofibers prepared by TEMPO-mediated oxidation of native cellulose, Biomacromolecules 8 (2007) 2485–2491, http://dx.doi.org/10.1021/bm0703970.
- [57] R. Shinoda, T. Saito, Y. Okita, A. Isogai, Relationship between length and degree of polymerization of TEMPO-oxidized cellulose nanofibrils, Biomacromolecules 13 (2012) 842–849, http://dx.doi.org/10.1021/ bm2017542.
- [58] H. Fukuzumi, T. Saito, A. Isogai, Influence of TEMPO-oxidized cellulose nanofibril length on film properties, Carbohydr. Polym. 93 (2013) 172–177, http://dx.doi.org/10.1016/j.carbpol.2012.04.069.